A phenomenological model for the flow resistance over submerged vegetation

Alexandra G. Konings,[1] Gabriel G. Katul,[1,2] and Sally E. Thompson[1]

Received 6 June 2011; revised 21 November 2011; accepted 9 January 2012; published 18 February 2012.

[1] The bulk velocity U_b in streams is conventionally estimated from Manning's equation, but difficulties remain in parameterizing the roughness coefficient n when the streambed is covered with vegetation. A two-layer velocity model is proposed to determine n and U_b for the submerged vegetation case. The modeled n is derived as a function of flow and vegetation properties that can be inferred from remote sensing platforms, such as canopy height, leaf area density, and flow depth. The main novelty in the proposed formulation is that the shear stress is related to the mean velocity profile by considering both ejective and sweeping motions by dominant eddies. The proposed model is tested against a large data set from the literature and is shown to perform well, particularly for rigid vegetation. Poorer model performance for flexible vegetation can be partially attributed to the shape of the assumed mean velocity profile. The roughness coefficient n is found to be robust to variations in the average spacing between canopy elements, allowing the model to be applied to heterogeneous canopies.

Citation: Konings, A. G., G. G. Katul, and S. E. Thompson (2012), A phenomenological model for the flow resistance over submerged vegetation, *Water Resour. Res.*, *48*, W02522, doi:10.1029/2011WR011000.

1. Introduction

[2] Methods to predict the bulk or area-averaged mean velocity U_b in streams commonly employ Manning's equation, which links U_b to channel slope S and hydraulic radius R through a single roughness coefficient n. In practice, values of n for a specific surface cover are selected using look-up tables [*Chow*, 1959]. Look-up table methods can be problematic for determining U_b in vegetated channels because vegetation characteristics substantially influence the mean velocity profile $\overline{u}(z)$, where z is the height from the channel bed and the overbar denotes Reynolds averaging. The vegetation structural properties on which $\overline{u}(z)$ depends vary in time and are not always known. However, remote sensing technologies do permit widespread characterization of vegetation attributes and flow characteristics. Interferometric synthetic aperture radar (InSAR) measurements allow for determination of variations in water surface elevation [*Alsdorf et al.*, 2007]. The future Surface Water and Ocean Topography (SWOT) satellite mission (recently approved as a NASA Decadal Survey Mission) will use InSAR and other instruments to provide estimates of water surface elevations with an accuracy on the scale of centimeters [*Durand et al.*, 2010]. Lidar methods can be used to characterize vegetation height (h_c) and leaf area density (a) for use as inputs to operational flood routing models [*Antonarakis et al.*, 2010; *Forzieri et al.*, 2010].

[3] Clearly, theoretical models to estimate U_b on the basis of these vegetation and water elevation properties can be decisive in advancing flood routing predictions. Although several such models have been proposed [e.g., *Wu et al.*, 1999; *Musleh and Cruise*, 2006; *Wilson*, 2007; *Yang and Choi*, 2010], these models have not generally taken advantage of what is known about the characteristics of the turbulent eddies that dominate momentum transport in vegetated systems. A model for U_b and n in channels with submerged vegetation is proposed here by extending the recent theoretical treatment of *Gioia and Bombardelli* [2002]. In this paper, a phenomenological approach is used to describe the momentum transfer at the canopy top on the basis of characterizing the dominant eddies, thereby closing the channel-wide momentum budget. In doing so, the effects of ejections and sweeps on momentum transfer associated with the eddies are simultaneously accounted for. Ejections occur when $u' < 0$ and $w' > 0$ and sweeps occur when $u' > 0$ and $w' < 0$ [*Robinson*, 1981], where $u = \overline{u} + u'$ and $w = \overline{w} + w'$ are the instantaneous streamwise and vertical velocities and primed quantities are excursions from the Reynolds-averaged quantities (indicated by overbar throughout).

[4] The proposed model is tested against (1) a large data set of measured values of n and U_b from the literature and (2) an existing two-layer model of flow in vegetation channels with regularly spaced rod elements [*Huthoff et al.*, 2007]. The principal differences between the model proposed here and that of Huthoff et al. are that the proposed model accounts for the momentum contributions generated by ejections and explicitly includes constraints imposed on the eddy sizes on the basis of their ability to penetrate the canopy, both features excluded in the model of *Huthoff et al.* [2007].

[1] Nicholas School of the Environment, Duke University, Durham, North Carolina, USA.
[2] Department of Civil and Environmental Engineering, Duke University, Durham, North Carolina, USA.

0043-1397/12/2011WR011000

2. Model Description

[5] In section 2 the model for n and U_b is derived for the submerged vegetation case. The phenomenological approach introduced by *Gioia and Bombardelli* [2002] for cases where the channel roughness height is small (referred to as the rough boundary layer formulation) is first summarized to illustrate the origins of the model structure. A model aquatic canopy is then introduced, and its properties are used to adapt the rough boundary layer formulation to a channel covered with vegetation. The entire derivation for the vegetated channel model is shown.

2.1. The Rough Boundary Layer Formulation

[6] *Gioia and Bombardelli* [2002] used a phenomenological approach to derive the turbulent shear stress (τ) at the channel bed when the channel roughness height is small relative to h_w. *Gioia and Chakraborty* [2006] and *Gioia et al.* [2010] also used a similar phenomenological model to quantify how variations in friction factor and mean velocity profile are impacted by variations in Reynolds number in pipe flow. In this approach, the roughness elements were assumed to have a length scale h_0. The τ was assumed to be dominated by eddies that straddle the coves between successive roughness elements at the wall surface. The projection of this eddy morphology is a sphere whose radius is h_0 centered on the plane tangent to the roughness elements and parallel to the bottom. The dominant eddy shape and channel system are illustrated in Figure 1. The τ from this eddy depends on the velocities tangent (v_t) and normal (v_n) to the surface,

$$\tau \sim \rho_w |\overline{v_t v_n}|, \tag{1}$$

where ρ_w is the density of water. The v_t depends on the difference between the velocity at the top of the eddy, which scales with U_b (in a single-layer model) and the velocity at the bottom of the eddy, which is assumed to be negligible relative to U_b because of the no-slip boundary condition. Thus, $v_t \sim (U_b - 0)$. The v_n is the characteristic velocity bounding the eddy of size h_0 and normal to the surface. The magnitude of this velocity is characterized by the structure function $v_n(h_0) = \left(\overline{[w'(x+h_0) - w'(x)]^2}\right)^{1/2}$, such that $v_n = \overline{(\Delta w(h_0))^2}^{1/2}$. For an eddy of radius h_o, *Gioia and Bombardelli* [2002] used the Kolmogorov four-fifths scaling law for the inertial subrange to estimate $v_n(h_0)$, which is given as [e.g., *Kolmogorov*, 1941; *Tennekes and Lumley*, 1972; *Frisch*, 1995]

$$v_n^3 = \overline{(\Delta w)^3} = -\frac{4}{5}\epsilon h_0, \tag{2}$$

where ϵ is the rate of dissipation of turbulent kinetic energy (TKE). This four-fifths scaling law is exact for locally homogeneous and isotropic turbulence, which may not characterize the dominant eddy here. If the Kolmogorov four-fifths scaling law is assumed to hold without any further modifications arising from TKE production or viscous dissipation, then equation (2) holds even for eddies extending throughout h_w. Such eddies have a radius commensurate with the hydraulic radius R (equal to $\frac{h_w B}{B+2h_w}$ for rectangular channels, where B is the channel width). The structure function of those eddies that scale with R at $z = h_0$ can be written as

$$\overline{(\Delta w(R))^2} = 2\overline{\sigma^2}(1 - \rho(R)), \tag{3}$$

where σ is the variance of the turbulent velocity, and ρ is its autocorrelation function. If the integral length scale of the turbulent velocity is smaller than h_w, then $\rho(R) \simeq 0$. As

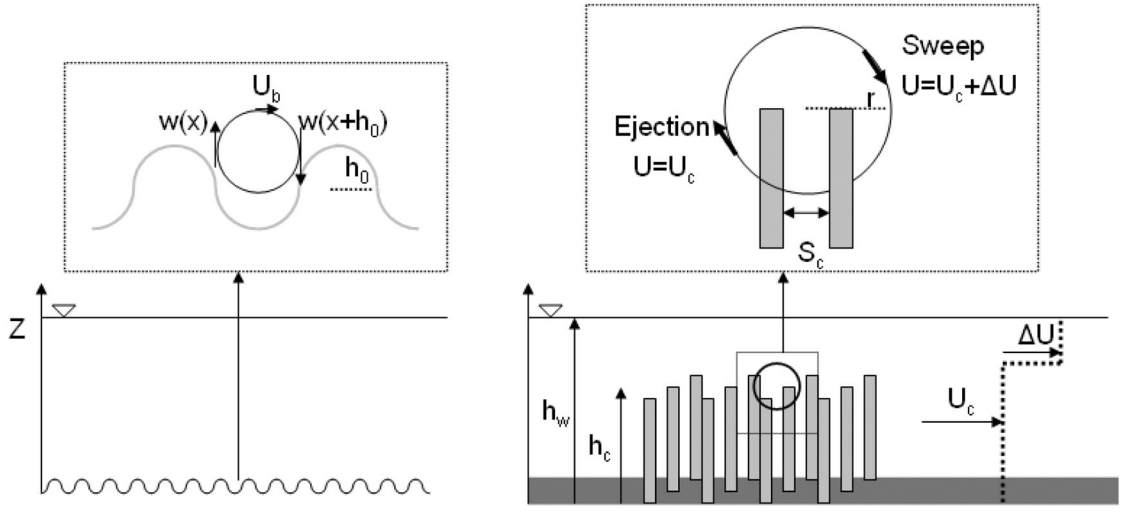

Figure 1. Schematic representation of the canopy and dominant eddy configuration. (left) The dominant eddies for the rough boundary layer formulation, which straddle the space between the roughness elements of radius h_0. The tangential velocity scale v_t associated with these eddies is U_b since there is no finite velocity at the bottom of the eddy. (right) A model for dominant eddies shown for aquatic vegetation. In this case, both ejections (associated with $U = U_c$, the velocity in the canopy) and sweeps (associated with $U = U_c + \Delta U$, the velocity above the canopy) contribute a finite velocity to v_t.

a result, $\overline{(\Delta w(R))^2} \sim 2\sigma^2$, a key assumption of *Gioia and Bombardelli* [2002]. Since the variance of the velocity scales as U_b^2, $\overline{(\Delta w(R))^2} \sim U_b^2$. From Kolmogorov's theory, then

$$\overline{(\Delta w(R))^2} \sim U_b^2 \sim \epsilon^{2/3} R^{2/3}, \tag{4}$$

and for the third-order structure function,

$$\begin{aligned} \overline{(\Delta w(R))^3} &\sim U_b^3 \sim \epsilon^{3/3} R^{3/3} \\ &\sim U_b^3 \sim \epsilon R. \end{aligned} \tag{5}$$

Combining equations (2) and (5) allows the estimation of v_n and $\frac{\tau}{\rho_w}$ as

$$v_n \sim U_b \left(\frac{h_0}{R}\right)^{1/3}. \tag{6}$$

Using equation (1),

$$\frac{\tau}{\rho_w} \sim U_b U_b \left(\frac{h_0}{R}\right)^{1/3}. \tag{7}$$

Assuming a uniform h_w and negligible wind shear stress at the channel surface, applying a force balance results in $\tau/\rho_w = gRS$, where g is the gravitational acceleration. Combining this with equation (7) results in

$$U_b \sim \left(\frac{h_0}{R}\right)^{-1/6} \sqrt{gSR}. \tag{8}$$

which recovers Manning's equation if $n^{-1} \sim h_0^{-1/6}\sqrt{g}$. The exponent 1/6 for h_0 is the typical "Strickler" scaling, and the $g^{-1/2}$ scaling has been derived or used by a number of studies [*Chow*, 1959; *Carr*, 1979; *Komar*, 1979; *Katul et al.*, 2002].

2.2. The Submerged Canopy Formulation

[7] The approach above can be extended to determine U_b of a submerged aquatic canopy, also illustrated in Figure 1. The canopy consists of cylindrical elements of diameter d and height h_c. The cylindrical canopy elements have a leaf area density a, defined as the canopy frontal area per volume. Its mean value can be determined from an "equivalent" leaf area index (LAI) using $a = \mathrm{LAI}/h_c$. The density of the canopy elements in the channel bed, defined as the number of stems per unit area, is n_d, such that the average spacing between canopy elements is $S_c = n_d - d$. The drag exerted by the canopy is represented by a constant drag coefficient C_d. As before, the flow in the channel has a depth h_w, with $h_w > h_c$. The submergence depth of the vegetation can be defined by the dimensionless height $\alpha = h_c/h_w < 1$. A two-layer velocity model is now assumed on the basis of the fact that the average velocity in the canopy is finite but substantially lower than the average velocity above the canopy for dense canopies [e.g., *Nepf and Vivoni*, 2000]. The velocity is assumed to have a constant average value within the canopy U_c, and a constant average value above it, with a discontinuity of size ΔU occurring at the canopy top. The flow velocity above the canopy is therefore $U_c + \Delta U$. Assuming α is known, the U_b is given by,

$$U_b = U_c + (1 - \alpha)\Delta U. \tag{9}$$

[8] As before, the shear stress at the top of the canopy (τ_c) is assumed to be dominated by eddies of a single optimal size (s) most efficient at transferring momentum. Such a dominant eddy is centered at the top of the canopy, as illustrated in Figure 1. As with the derivation of τ, τ_c depends on v_n and v_t. The v_t again depends on the difference between the velocity at the top of the eddy, now $U_c + \Delta U$, and the velocity at the bottom of the eddy, now U_c. Therefore, $v_t \sim \Delta U$. As before, v_n is the characteristic velocity of eddies of size s (u_s) and the Kolmogorov four-fifths law can be used so that

$$u_s = U_b \left(\frac{s}{h_w}\right)^{1/3}. \tag{10}$$

[9] The use of the four-fifths law assumes that the Kolmogorov model of turbulence is an accurate description of the flow at the canopy top. Some evidence exists to support this assumption. Figure 2 presents an idealized version of vertical velocity energy spectra measured by *Poggi et al.* [2004a, Figure 5b] in a flume with submerged steel rods acting as canopy elements. The spectrum at a height near the canopy top ($z/h_c = 1.1$) is close to the expected Kolmogorov spectrum in terms of scaling laws. Inside the canopy, the spectrum is complicated by numerous factors including wake production at Strouhal frequencies commensurate with the generation of Von Karman streets, shear production at larger scales, and the lack of Kolmogorov scaling often used in delineating the inertial subrange.

[10] Equation (10) also assumes that the h_w length scale is within the inertial subrange at $z = h_c$. The canopy top spectrum in Figure 2 shows that while the inertial subrange extends to h_c at $z/h \sim 1$, it does not extend to h_w. However, the spectrum at $z/h \sim 1$ resembles one with conventional descriptions of the modulations to the K41 spectrum by production and dissipation. Appendix A explores the use of a canonical spectrum with these modulations (that of *Gioia et al.* [2010], which resembles the spectrum at $z/h \sim 1.9$). Accounting for the energetic and dissipative regimes only has a minor effect on the predicted n, suggesting that the use of Kolmogorov's four-fifths law in describing u_s is a reasonable assumption up to scales commensurate with h_w, at least at the canopy top. As shown in Figure 2, the use of the four-fifths law is not accurate for describing flow deeper in the canopy; hence using this approach is questionable when describing turbulent stresses at some arbitrary level inside the canopy.

[11] To evaluate u_s in equation (10), the size of the eddy dominating the shear stress must be known. The shear stress is dominated by the largest possible eddy centered at the top of the canopy. Both horizontal and vertical length scales can limit the eddy size. Vertically, the eddy radius s is constrained by the depth of water above the canopy

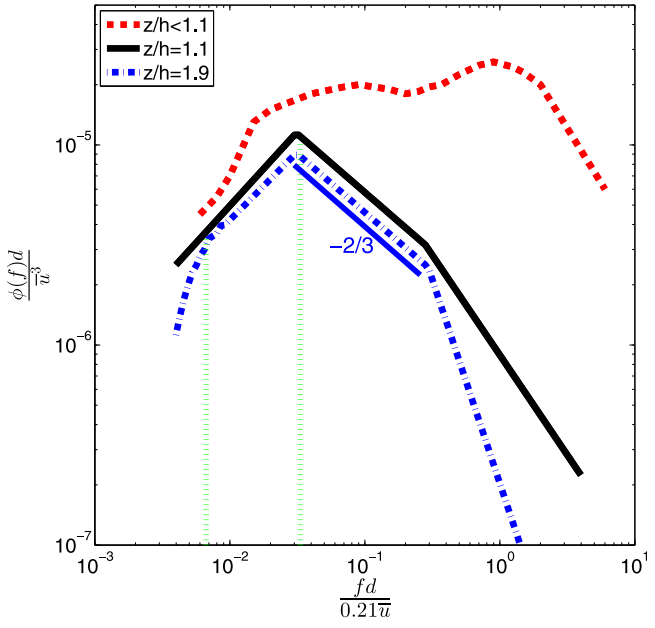

Figure 2. Idealized version of the energy spectra measured at different heights in *Poggi et al.* [2004a]. The spectra are premultiplied by the wave number, such that a slope of $-2/3$ corresponds to the slope of $-5/3$ $(= -2/3 - 1)$ in the usual Kolmogorov spectrum. The black solid line is the spectrum right above the canopy top, at $z/h = 1.1$, while the red dashed line represents the spectrum deep within the canopy, at $z/h < 1$. The blue dash-dotted line is the spectrum at a height well above the canopy top. The green vertical lines correspond to the frequencies associated with the water depth h_w and the canopy height h_c in the experiments of *Poggi et al.* [2004a], respectively.

$h_w(1-\alpha)$ and by the depth to which the eddies can effectively penetrate the canopy. The penetration depth is conventionally defined as the depth at which the Reynold's stress is 10% of the top of the canopy value [*Nepf and Vivoni*, 2000]. Across a wide range of experiments, *Nepf et al.* [2004] found that the penetration depth δ was given by

$$\delta = \begin{cases} \dfrac{0.21}{C_d a}, & (C_d a h_c)^{-1} \le 4, \\ 0.85 h_c, & (C_d a h_c)^{-1} > 4. \end{cases} \tag{11}$$

The limiting vertical length scale is given by $r = \min(\delta, h_w - h_c)$. The limiting horizontal length scale is given by $B/2$. Since the canopy eddies do not continuously span the channel laterally, not all momentum is necessarily absorbed over the distance between canopy elements S_c. The $B/2$ is therefore expected to be a more appropriate horizontal length scale than S_c. In the derivation here, relatively wide channels are assumed so that $h_w < B$. As a result, $r < B$ and $s = r$. This eddy length scale is supported by the measurements of *Ghisalberti* [2010].

[12] The phenomenological description of τ_c can be used to close the momentum budget by employing a force balance on the layer of flow above the canopy. Assuming the flow is steady and uniform and that dispersive fluxes are small enough to be neglected [*Poggi et al.*, 2004b], the force of gravity on the water above the vegetation canopy is balanced by the shear stress produced at the top of the canopy so that

$$\rho_w g(h_w - h_c)S = \tau_c + \tau_w, \tag{12}$$

where τ_w is the drag on the channel walls above h_c, which is assumed to be small relative to the drag at the top of the canopy. Evaluating the shear stress in equation (12) and simplifying gives

$$g(h_w - h_c)S = K_\tau \left(\frac{r}{h_w}\right)^{1/3} U_b \Delta U, \tag{13}$$

where K_τ is a constant of proportionality.

[13] Applying a force balance to the entire channel (using the same assumptions as in equation (12)) provides an equation for U_c given as

$$\rho_w g h_w S = \rho_w \frac{1}{2} C_d a h_c U_c^2 + \tau_b(0) + \tau_w(0), \tag{14}$$

where the right-hand side is the drag force created by the canopy elements and the drag at the canopy bed τ_b and on the channel walls τ_w. The $\tau_b(0)$ and τ_w are assumed here to be negligible relative to the canopy drag. With this simplification,

$$U_c = \sqrt{\frac{2gS}{\alpha C_d a}} = \sqrt{\frac{2gSl_c}{\alpha}}. \tag{15}$$

The quantity $l_c = (C_d a)^{-1}$ is known as the adjustment length scale and is used in canopy turbulence studies to parameterize the loss of turbulent kinetic energy from advecting eddies due to their dissipation by the canopy drag elements [*Finnigan*, 2000; *Belcher et al.*, 2003].

[14] Equations (9), (13), and (14) form a system of three equations with three unknowns, U_b, U_c, and ΔU. Combining the three equations leads to a single quadratic equation for U_b,

$$U_b^2 - \sqrt{\frac{2gSl_c}{\alpha}} U_b - (1-\alpha)\frac{g(h_w - h_c)S}{K_\tau}\left(\frac{h_w}{r}\right)^{1/3} = 0. \tag{16}$$

Substituting Manning's equation provides a single quadratic equation for n:

$$(1-\alpha)\frac{g(h_w - h_c)}{K_\tau R^{2/3}}\left(\frac{h_w}{r}\right)^{1/3} n^2 + \sqrt{\frac{2gl_c}{\alpha}} n - R^{2/3} = 0. \tag{17}$$

Equation (17) has only a single positive root. Unlike U_b, n is independent of S, as expected. Note that for a vegetated channel, the Strickler scaling is not recovered when h_c goes to 0 since the bed stress τ_b is assumed zero. If τ_b is finite and accounted for, the Strickler scaling will be recovered for the h_o of the channel bed via the conventional arguments of *Gioia and Bombardelli* [2002].

3. Data Sets

[15] The model was tested using a data set consisting of a large range of laboratory measurements of flows with

submerged vegetation from the literature. It includes the data sets listed by *Poggi et al.* [2009] and *Cheng* [2011]. One hundred sixty-eight experiments in the data set examine rigid canopy elements [*Fenzl*, 1962; *Dunn et al.*, 1996; *Stone*, 1997; *Meijer and van Velzen*, 1999; *Lopez and Garcia*, 2001; *Ghisalberti and Nepf*, 2004; *Poggi et al.*, 2004a; *Murphy et al.*, 2007; *Liu et al.*, 2008; *Nezu and Sanjou*, 2008; *Yang and Choi*, 2009; *Cheng*, 2011], and 67 experiments considered flexible vegetation [*Dunn et al.*, 1996; *Carolla et al.*, 2002; *Jarvela*, 2005; *Ciraolo and Ferreri*, 2007; *Kubrak et al.*, 2008; *Yang and Choi*, 2009]. When $C_d a h_c < 0.2$, eddies may penetrate to the channel bed [*Nepf et al.*, 2007], which would invalidate the assumption of a nonnegligible bed stress in equation (14). Because the model is only valid when $C_d a h_c > 0.2$, only experiments that meet this condition are included.

[16] The drag coefficient was not measured in all of the studies used. Wherever an estimate of C_d was used in the original study, that value was used here as well. When C_d is unknown, $C_d = 1.13$ was used. This was the mean value measured experimentally by *Dunn et al.* [1996], matching analytical estimates of *Li and Shen* [1973]. This is also the value used by *Lopez and Garcia* [2001].

[17] Flexible vegetation elements can deflect, changing the geometry of the problem. Therefore, the rigid and flexible vegetation cases are considered separately. For flexible vegetation, h_c is assumed to be the reported deflected canopy height. The experiments cover a wide range of n (0.018–0.139 for rigid vegetation and 0.011–0.130 for flexible vegetation) that approximately spans the entire range of n values typically assumed for natural channels [*Chow*, 1959]. The data set also spans a range of values for the Reynolds number, α, S, and R. A table with parameter values for each of the data points is included as auxiliary material.[1] A best fit value is found separately for the scaling parameter K_τ for rigid and flexible canopies.

4. Results

[18] *Huthoff et al.* [2007] was the first to apply the methodology of *Gioia and Bombardelli* [2002] to derive a two-layer velocity model for vegetated channels, using an approach similar to that employed here. Two crucial differences exist between the model of *Huthoff et al.* [2007] and the one proposed here: (1) Huthoff et al. argued that velocity fluctuations tangent to the streamflow are proportional to the average velocity above the canopy rather than to the difference in velocity above and below the canopy top, as argued here, and (2) the length scale used by Huthoff et al. is proportional to the horizontal spacing between regularly distributed canopy elements, rather than depending on the penetration depth or $h_w - h_c$ as argued here. Because the conceptual reasoning behind the two models is similar, the performance of both models on the data set is compared.

4.1. Rigid Canopies

[19] The best fit value of the (dimensionless) K_τ is 0.21 ± 0.04 for the rigid canopies. This estimate is robust with respect to the number of data points used to estimate its value. When half of the data points were randomly selected and used to estimate K_τ, its value did not change markedly. This provides confidence that the estimate of K_τ is robust and can be applied to other conditions.

[20] Figures 3a and 3b compare measured and predicted values of n and U_b of the rigid canopy data set for the proposed model and for the model of *Huthoff et al.* [2007]. Both models perform reasonably well in estimating both variables. Within the data set of *Stone* [1997], four groups of experiments exist for which all runs have the same canopy density, canopy height, and flow depth and width. Only the channel slope (and flow rate) differs between runs. Because n is independent of S, the estimated n is the same for each of the runs in a group. However, the measured n varies between estimates. These groups are identifiable as the clusters of points that form a horizontal line in Figure 3a. The estimates of U_b for the same data points do not have a qualitatively different error structure than the rest of the data set, suggesting that the (in)sensitivity of the n estimates to the channel slope S is more incorrect than the sensitivity of the U_b estimates to S. Since the only difference between the models of n (equation (17)) and U_b (equation (16)) is in the application of Manning's equation, this in turn suggests that the variation in measured n for these runs occurs because of an S dependence in n, rather than because of some other variable factor between the different runs that is not accounted for here.

[21] Table 1 shows the coefficient of determination, root-mean-square error (RMSE), and bias for each model and variable combination. The model proposed here has a lower root-mean-square error than the model of *Huthoff et al.* [2007]. Although the eddy length scale and the ejection contribution used by the two models differ, errors associated with both models are broadly similar. Experiments with relatively high error in one model often have relatively high errors for the other. This can be explained by noting that the model performance is relatively insensitive to the length scale used for r (i.e., the limiting vertical length scale). The root-mean square distance between estimates of n with eddy length scale of r and estimates using an eddy length scale equal to S_c is only 0.0014 s m^{-3}.

[22] The model is relatively insensitive to the precise value of the drag coefficient used. When using the value $C_d = 1.13$ instead of the reported C_d when available, no estimate of n changed by more than 15% (not shown). In general, the drag coefficient may depend on the exact variation of canopy properties with height from the channel bottom, which may not be known and can be difficult to estimate for a large range of species without detailed measurements. The model's insensitivity to C_d thus significantly improves the range of its applicability for practical purposes.

4.2. Flexible Canopies

[23] For flexible canopies, the best fit value of K_τ is lower at 0.74 ± 0.016. The reduction in K_τ is expected because vegetation deflection in flexible canopies often leads to drag reductions. The model performance for cases of flexible canopies is also presented in Figure 3 and summarized in Table 1. Not surprisingly, the models perform worse than for the rigid case. The deflection of flexible

[1] Auxiliary materials are available in the HTML. doi:10.1029/2011WR011000.

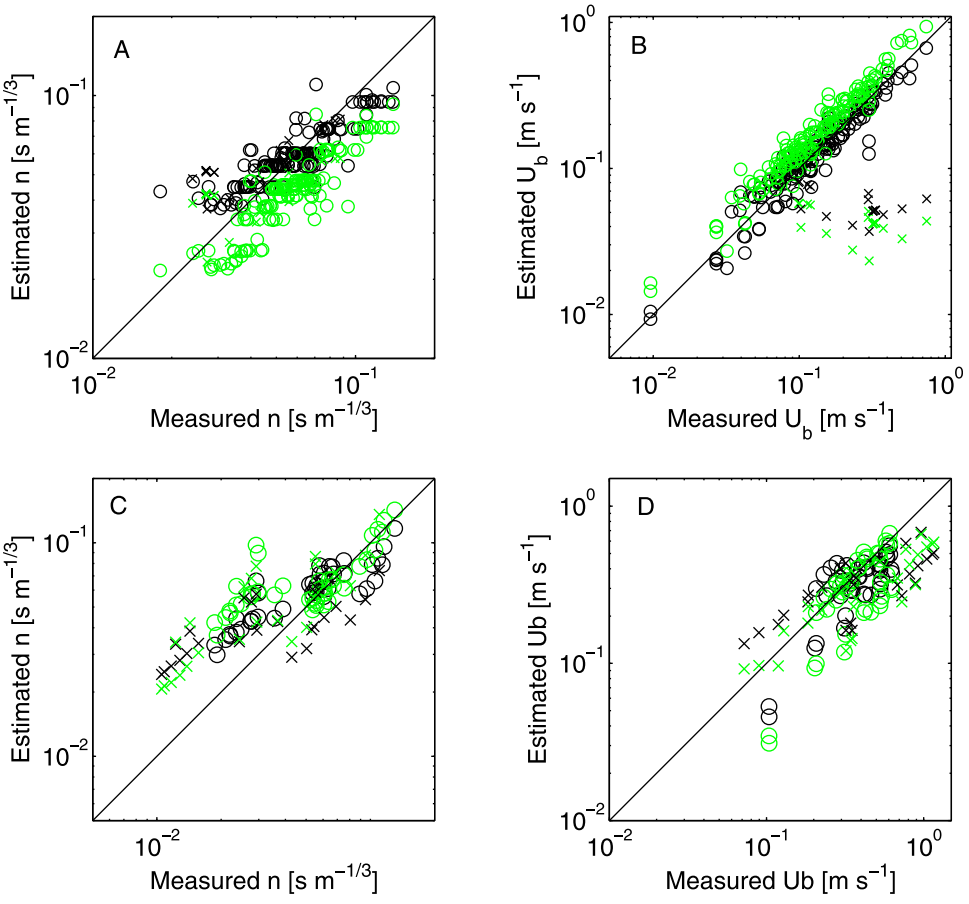

Figure 3. Comparison between predicted and measured (a) Manning's roughness coefficient n and (b) bulk velocity U_b for the laboratory experiments with rigid canopy elements. (c and d) The same as Figures 3a and 3b, respectively, but showing the laboratory experiments with flexible canopy elements. Black symbols represent predictions of the proposed model, while green symbols represent those from the model of *Huthoff et al.* [2007]. Crosses represent points for which the drag coefficient was not studied in the original experiment and for which its value was assumed to equal 1.13 as in the work by *Dunn et al.* [1996].

vegetation affects not only the canopy height and drag, but also the leaf area density and any coupling between the flow inside and above the vegetation. This is not explicitly accounted for in either of the two models.

Table 1. Comparison Between Measured and Modeled U_b and n for Rigid and Flexible Canopies[a]

	R^2	RMSE	Bias	m	b
		Rigid Canopy			
n, Huthoff et al.	0.80	0.019	0.81	0.55	0.013
n, proposed	0.82	0.012	1.09	0.57	0.026
U_b, Huthoff et al.	0.90	0.068	1.29	1.18	0.010
U_b, proposed	0.90	0.046	0.96	0.80	0.020
		Flexible Canopy			
n, Huthoff et al.	0.65	0.021	1.51	0.69	0.027
n, proposed	0.65	0.019	1.33	0.50	0.028
U_b, Huthoff et al.	0.51	0.21	0.79	0.46	0.12
U_b, proposed	0.44	0.21	0.89	0.34	0.19

[a]The coefficient of determination (R^2), the root-mean-square error (RMSE), and the relative error or bias (= (measured − modeled)/measured) are shown. Parameters m and b are the slope and intercept of a robust linear regression of the predicted against the measured values with a bilinear weighting scheme. Huthoff et al. refers to the work by *Huthoff et al.* [2007].

[24] As a result of the failure to account for canopy deflection, the assumption of constant leaf area density, drag coefficient, and canopy layer velocity U_c is no longer realistic in flexible canopies. In reality, U_c increases with height and changes during the deflection cycle. The tangent velocity scale v_t is higher than U_c at the bottom of the eddy, so that the value of v_t used in the eddy momentum transfer, calculated as $(U_c + \Delta U) - U_c = \Delta U$, is too high. Equation (13) therefore predicts a U_b that is too low, and the estimate of n is high. This is reflected in Table 1 through the bias in n. The magnitude of this error is expected to depend on how far the dominant eddy can penetrate into the canopy, and therefore on the ratio of r to h_c. With the linear model for r assumed here, $r/h_c = 0.21 l_c/h_c$ for sufficiently dense data sets that are not limited by the flow depth above the canopy ($r = \delta$). Figure 4 shows the magnitude of the absolute error as a function of $0.21 l_c/h_c$ for such experiments. The error decreases with $0.21 l_c/h_c$, suggesting that the variability of U_c with height is a possible source of error for the model. The data in Figure 4 do not collapse to a single line because the magnitude of other errors depends on flow conditions as well. Nevertheless, the behavior is roughly similar for each individual data set

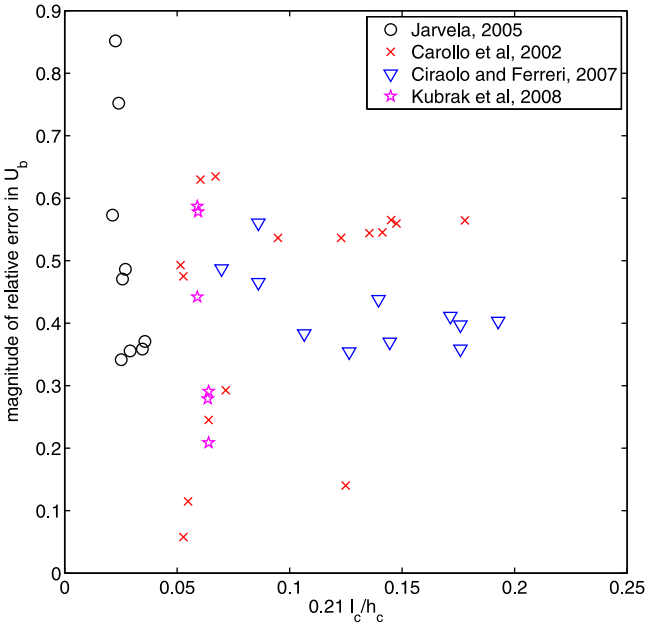

Figure 4. The magnitude of relative error in the bulk velocity U_b (the magnitude of the error in predicted U_b, normalized by the observed value) as a function of $0.21l_c/h_c$, the ratio of the predicted r/h_c for different data sets. Only data with flexible canopies for which $r/h_c = 0.21l_c/h_c$ are shown. Thus, very sparse data sets (for which $(C_d a h_c)^{-1} > 4$) and data sets for which the flow depth above the canopy is limiting ($h_w - h_c < \delta$) are not shown.

with flexible canopies, except the data of *Carolla et al.* [2002]. Unlike other data sets, that of *Carolla et al.* [2002] uses a variety of species as canopy elements, likely complicating the model behavior and sensitivities. Note that, with the exception of data from *Jarvela* [2005] and *Carolla et al.* [2002], most estimates have a relative error of less than 0.5, a reasonable value given the large range of tested n.

[25] As canopy density increases, the system begins to act similarly to flow over a permeable wall of height h_c. The flow rate below the depth to which the eddy penetrates becomes essentially zero. The contribution of U_c to equation (9) should then be less, such that the model used here overestimates U_b and underestimates n. This prediction is supported by the model underestimating n for the nine data points of *Jarvela* [2005], which are by far the least porous data points measured (taking canopy porosity as $1 - \frac{\pi}{4}ad$, [*Nepf et al.*, 2004]). The velocity profiles observed in the study of *Jarvela* [2005] are near zero in much of the canopy, suggesting that the lack of flow is the dominant source of error for these nine experiments.

5. Conclusions

[26] The model presented here phenomenologically links turbulence theory with vegetation properties to make predictions about flow in densely vegetated channels. The model can be applied to both rigid and flexible vegetation, but performs better for the rigid case as expected. The discrepancy in performance is attributed to the fact that the model does not fully account for the variability in the deflected vegetation height between sweeps and ejections [*Ghisalberti and Nepf*, 2006] or for the effect of the canopy deflection on the flow. When the vegetation canopy is flexible, C_d and U_c can vary significantly with height and U_b, which may contribute to prediction errors for flexible canopies. Vegetation and vegetation proxies are not perfectly cylindrical and may include leaves and other elements that cause significant variations in C_d and a with height. This amplifies the effects of any variability with height in U_c.

[27] To use a phenomenological approach for describing the canopy shear stress (equation (1)), two quantities must be determined: the eddy velocity scaling v_n and v_t and the proportionality between the eddy velocities and the shear stress, given by K_τ. The value of K_τ estimated here is smaller than values of K_τ proposed for similar phenomenological models [*Gioia and Chakraborty*, 2006; *Gioia et al.*, 2010], both in the case of rigid and of flexible canopies. Simulation studies can provide further insight into the value and dependence of K_τ on vegetation properties. Significant progress has been made in recent years on simulating the dynamic two-way interaction between deflecting plants and flow using large-eddy simulation studies [*Dupont et al.*, 2010], and other approaches [*de Langre*, 2008]. These approaches may also be used to determine the variables that might impact K_τ, including the density and the elastic properties of the vegetation.

[28] The magnitude of the bias and the RMSE for the model proposed here are lower than those generated by the model of *Huthoff et al.* [2007] for both rigid and flexible canopies. One of the key differences between the model of *Huthoff et al.* [2007] and that presented here is the choice of length scale as the scaling factor for the eddy velocity. When applied to rigid canopies, the model is essentially insensitive to the choice of a vertical (r) or horizontal (S) length scale. Though the choice of the eddy length scale influences the estimates of n and U_b for flexible canopies, the effect is still much smaller than the effect of the choice of v_t. Physically, the proposed model suggests ejections are nonnegligible contributors to the shear stress at the top of the canopy. The small sensitivity to n and U_b is not surprising, because equations (16) and (17) show that U_b and n depend only on $s^{1/3}$. This one-third power results from the use of Kolmogorov's four-fifths law for scaling the eddy velocity and has the effect of dampening variations in the length scale. Despite this dampening effect, a vertical length scale performs slightly better than using a horizontal length scale.

[29] Finally, the fact that the model presented here allows prediction of n and U_b independently of the spacing between canopy elements is a considerable advantage. It allows the model to be applied to heterogeneous canopies that do not have a unique spacing width, a necessary step toward bridging the gap between measurements in laboratory flows and predictions for natural channels.

Appendix A

[30] The assumption that the turbulent spectrum is entirely in the inertial range can be relaxed to derive a more complete equation for u_s. This equation is derived

here in analogy to work of *Gioia and Chakraborty* [2006]. The u_s depends on the energy spectrum according to

$$u_s^2 = \int_0^s \frac{E(\sigma)}{\sigma^2} d\sigma, \tag{A1}$$

where σ is a length scale, and $E(\sigma)$ is given by [*Pope*, 2000]

$$E(\sigma) = A\epsilon^{2/3}\sigma^{5/3} c_d(\sigma) c_e(\sigma), \tag{A2}$$

where c_d and c_e are correction formulas for the reductions in the dissipative and energetic regions of the spectrum, respectively. A is a dimensionless constant and has a value of about 1.5 [*Tennekes and Lumley*, 1972, p. 271]. The $c_d(\sigma) = \exp(-\beta\eta/\sigma)$, where $\beta = 2.1$ scales the exponential and $\eta = \nu^{3/4}\epsilon^{-1/4}$ is the viscous length scale, with ν the kinematic viscosity of water. The value of η is determined below. The c_d decreases exponentially from one as σ decreases and nears the viscous length scale. The $c_e(\sigma) = (1 + \gamma(\sigma/R)^2)^{-17/6}$, where $\gamma = 3.715$ is a scaling constant [*Pope*, 2000, p. 232–234]. The $c_e \approx 1$ for most σ but increases as σ nears R.

[31] Kolmogorov's four-fifths law is applied at the channel-wide scale to determine ϵ as before, $v_n^3 = (4/5)\epsilon R$. Considering the second-order structure function of velocity and assuming that the correlation function of the velocity fluctuations u' goes to zero for large eddies, $v_n^2 \sim \overline{u'^2}$. Since the velocity fluctuations and the depth-averaged velocity scale with the same canopy boundary conditions, it is reasonable to assume $\overline{u'^2} \sim U_b^2$. Defining the constant of proportionality between the two quantities to be K_u, $v_n = K_u U_b$. Thus, $\epsilon = 5/4K_u^3 U_b^3/R$, which allows calculation of η as

$$\eta = \nu^{3/4}\left(\frac{5K_u^3 U_b^3}{4R}\right)^{-1/3}. \tag{A3}$$

[32] Combining these definitions and substituting into equation (A1) leads to

$$u_s^2 = \left[\left(\frac{5}{4}\right)^{2/3}\frac{A}{R^{2/3}}\int_0^s \sigma^{-1/3}\exp\left(\frac{-\beta\eta}{\sigma}\right)(1+\gamma(\sigma/R)^2)^{-17/6}d\sigma\right] \times K_u^2 U_b^2. \tag{A4}$$

Note that unlike in equation (6), u_s no longer depends linearly on U_b because ϵ depends (slightly) on U_b. This equation for u_s has an additional fitting parameter K_u. If the equation is combined with the two-layer flow model described above, and an optimal fitting value of K_u is used, no estimate of n changes by more than 5%.

[33] **Acknowledgments.** The authors gratefully acknowledge useful discussions with June Yin and helpful comments and suggestions from the anonymous reviewers. The first author was supported through the National Science Foundation (NSF) Graduate Research Fellowship program. G. G. Katul and S. E. Thompson acknowledge support from NSF through grants (NSF-EAR-1013339, NSF-AGS-1102227, and NSF-CBET-103347), the United States Department of Agriculture (2011-67003-30222), and the U.S. Department of Energy (DOE) through the office of Biological and Environmental Research (BER) Terrestrial Ecosystem Science (TES) Program (DE-SC0006967).

References

Alsdorf, D., E. Rodriguez, and D. Lettenmaier (2007), Measuring surface water from space, *Rev. Geophys.*, *45*, RG2002, doi:10.1029/2006RG000197.

Antonarakis, A., K. Richards, J. Brasington, and E. Muller (2010), Determining leaf area index and leafy tree roughness using terrestrial laser scanning, *Water Resour. Res.*, *46*, W06510, doi:10.1029/2009WR008318.

Belcher, S., N. Jerram, and J. Hunt (2003), Adjustment of a turbulent boundary layer to a canopy of roughness elements, *J. Fluid. Mech.*, *488*, 369–398.

Carolla, F., V. Ferro, and D. Termini (2002), Flow velocity measurements in vegetated channels, *J. Hydraul. Eng.*, *128*, 664–673, doi:10.1061/(ASCE)0733-9429(2002)128:7(664).

Carr, M. H. (1979), Formation of martial flood features by release of water from confined aquifers, *J. Geophys. Res.*, *84*, 2995–3007.

Cheng, N. (2011), Representative roughness height of submerged vegetation, *Water Resour. Res*, *47*, W08517.

Chow, V. (1959), *Open-Channel Hydraulics*, 680 pp., McGraw-Hill, New York.

Ciraolo, G., and G. B. Ferreri (2007), Log velocity profile and bottom displacement for a flow over a very flexible submerged canopy, paper presented at 32nd Congress: Harmonizing the Demands of Art and Nature in Hydraulics, Int. Assoc. of Hydraul. Eng. and Res., Venice, Italy.

de Langre, E. (2008), Effects of wind on plants, *Annu. Rev. Fluid Mech.*, *40*, 141–168, doi:10.1146/annurev.fluid.40.111406.102135.

Dunn, C., F. Lopez, and M. Garcia (1996), Mean flow and turbulence in a laboratory channel with simulated vegetation, *Hydraul. Eng. Ser. 51*, Hydrosyst. Lab., Dep. of Civ. Eng., Univ. of Ill. at Urbana-Champaign, Urbana.

Dupont, S., F. Gosselin, C. Py, E. de Langre, P. Hemon, and Y. Brunet (2010), Modelling waving crops using large-eddy simulation: Comparison with experiments and a linear stability analysis, *J. Fluid Mech.*, *652*, 5–44, doi:10.1017/S0022112010000686.

Durand, M., F. Lee-Lueng, D. Lettenmaier, D. Alsdorf, E. Rodriguez, and D. Esteban-Fernandez (2010), The Surface Water and Ocean Topography Mission: Observing terrestrial surface water and oceanic submesoscale eddies, *Proc. IEEE*, *98*, 766–779, doi:10.1109/JPROC.2010.2043031.

Fenzl, R. (1962), Hydraulic resistance of broad shallow vegetated channels, PhD thesis, Univ. of Calif., Davis.

Finnigan, J. (2000), Turbulence in plant canopies, *Annu. Rev. Fluid Mech.*, *32*, 519–571, doi:10.1146/annurev.fluid.32.1.519.

Forzieri, G., G. Moser, E. Vivoni, F. Castelli, and F. Canovaro (2010), Riparian vegetation mapping for hydraulic roughness estimation using very high resolution remote sensing data fusion, *J. Hydraul. Eng.*, *136*, 855–867, doi:10.1061/(ASCE)HY.1943-7900.0000254.

Frisch, U. (1995), *Turbulence*, 296 pp., Cambridge Univ. Press, Cambridge, U. K.

Ghisalberti, M. (2010), The three-dimensionality of obstructed shear flows, *Environ. Fluid. Mech.*, *10*, 329–343, doi:10.1007/s10652-009-9161-4.

Ghisalberti, M., and H. Nepf (2004), The limited growth of vegetated shear layers, *Water Resour. Res.*, *40*, W07502, doi:10.1029/2003WR002776.

Ghisalberti, M., and H. Nepf (2006), The structure of the shear layer in flows over rigid and flexible canopies, *Environ. Fluid. Mech.*, *6*, 277–301, doi:10.1007/s10652-006-0002-4.

Gioia, G., and F. Bombardelli (2002), Scaling and similarity in rough channel flows, *Phys. Rev. Lett.*, *88*(1), 014501, doi:10.1103/PhysRevLett.88.014501.

Gioia, G., and P. Chakraborty (2006), Turbulent friction in rough pipes and the energy spectrum of the phenomenological theory, *Phys. Rev. Lett.*, *96*, 044502, doi:10.1103/PhysRevLett.96.044502.

Gioia, G., N. Guttenberg, N. Goldenfeld, and P. Chakraborty (2010), Spectral theory of the turbulent mean-velocity profile, *Phys. Rev. Lett.*, *105*, 184501, doi:10.1103/PhysRevLett.105.184501.

Huthoff, F., D. Augustijn, and S. Hulscher (2007), Analytical solution of the depth-averaged flow velocity in case of submerged rigid cylindrical vegetation, *Water Resour. Res.*, *43*, W06413, doi:10.1029/2006WR005625.

Jarvela, J. (2005), Effect of submerged flexible vegetation on flow structure and resistance, *J. Hydrol.*, *307*, 233–241, doi:10.1016/j.jhydrol.2004.10.013.

Katul, G., P. Wiberg, J. Albertson, and G. Hornberger (2002), A mixing layer theory for flow resistance in shallow streams, *Water Resour. Res.*, *38*(11), 1250, doi:10.1029/2001WR000817.

Kolmogorov, A. (1941), Dissipation of energy under locally isotropic turbulence, *Dokl. Akad. Naukl. SSSR*, *32*, 16–18.

Komar, P. (1979), Comparisons of the hydraulics of water flows in Martian outflow channels with flows of similar scale on Earth, *Icarus*, *37*, 158–181.

Kubrak, E., J. Kubrak, and P. Rowinski (2008), Vertical velocity distributions through and above submerged, flexible vegetation, *Hydrol. Sci. J.*, *53*(4), 905–920, doi:10.1623/hysj.53.4.905.

Li, R., and H. Shen (1973), Effect of tall vegetations on flow and sediment, *J. Hydraul. Div. Am. Soc. Civ. Eng.*, *99*(5), 793–813.

Liu, D., P. Diplas, J. Fairbanks, and C. Hodges (2008), An experimental study of flow through rigid vegetation, *J. Geophys. Res.*, *113*, F04015, doi:10.1029/2008JF001042.

Lopez, F., and M. H. Garcia (2001), Mean flow and turbulence structure of open-channel flow through non-emergent vegetation, *J. Hydraul. Eng.*, *127*, 392–402, doi:10.1061/(ASCE)0733-9429(2001)127:5(392).

Meijer, D., and E. H. van Velzen (1999), Prototype scale flume experiments on hydraulic roughness of submerged vegetation, paper presented at 28th International Conference, Int. Assoc. of Hydraul. Eng. and Res., Graz, Austria.

Murphy, E., M. Ghisalberti, and H. Nepf (2007), Model and laboratory study of dispersion in flows with submerged vegetation, *Water Resour. Res.*, *43*, W05438, doi:10.1029/2006WR005229.

Musleh, F. A., and J. F. Cruise (2006), Functional relationships of resistance in wide flood plains with rigid unsubmerged vegetation, *J. Hydraul. Eng.*, *132*, 163–171, doi:10.1061/(ASCE)0733-9429(2006)132:2(163).

Nepf, H. M., and E. R. Vivoni (2000), Flow structure in depth-limited, vegetated flow, *J. Geophys. Res.*, *105*(C12), 28,547–28,557.

Nepf, H. M., B. White, A. Lightbody, and M. Ghisalberti (2004), Transport in aquatic canopies, in *Flow and Transport Processes With Complex Obstructions: Applications to Cities, Vegetative Canopies, and Industry*, edited by Y. Gayev and J. Hunt, pp. 221–250, Springer, Berlin.

Nepf, H., M. Ghisalberti, B. White, and E. Murphy (2007), Retention time and dispersion associated with submerged aquatic canopies, *Water Resour. Res.*, *43*, W04422, doi:10:1029/2006WR005362.

Nezu, I., and M. Sanjou (2008), Turbulence structure and coherent motion in vegetated canopy open-channel flows, *J. Hydro-environ. Res.*, *2*(2), 62–90.

Poggi, D., A. Porporato, L. Ridolfi, J. Albertson, and G. Katul (2004a), The effect of vegetation density on canopy sub-layer turbulence, *Boundary Layer Meteorol.*, *111*, 565–587, doi:10.1023/B:BOUN.0000016576.05621.73.

Poggi, D., G. Katul, and J. Albertson (2004b), A note on the contribution of dispersive fluxes to momentum transfer within canopies, *Boundary Layer Meteorol.*, *111*, 615–621, doi:10.1023/B:BOUN.0000016563.76874.47.

Poggi, D., C. Krug, and G. G. Katul (2009), Hydraulic resistance of submerged rigid vegetation derived from first-order closure models, *Water Resour. Res.*, *45*, W10442, doi:10.1029/2008WR007373.

Pope, S. (2000), *Turbulent Flows*, 771 pp., Cambridge Univ. Press, Cambridge, U. K.

Robinson, S. (1981), Coherent motions in the turbulent boundary layer, *Annu. Rev. Fluid Mech.*, *23*, 601–639.

Stone, B. (1997), Hydraulics of flow in vegetated channels, MS thesis, Clarkson Univ., Potsdam, N. Y.

Tennekes, H., and J. Lumley (1972), *A First Course in Turbulence*, 300 pp., MIT Press, Cambridge, Mass.

Wilson, C. (2007), Flow resistance models for flexible submerged vegetation, *J. Hydrol.*, *342*, 213–222, doi:10.1016/j.jhydrol.2007.04.022.

Wu, F., H. Shen, and Y. Chou (1999), Variation of roughness coefficients for unsubmerged and submerged vegetation, *J. Hydraul. Eng.*, *125*, 934–942.

Yang, W., and S. Choi (2009), Impact of stem flexibility on mean flow and turbulence structure in depth-limited open channel flows with submerged vegetation, *J. Hydraul. Res.*, *47*, 445–454.

Yang, W., and S. Choi (2010), A two-layer approach for depth-limited open-channel flows with submerged vegetation, *J. Hydraul. Res.*, *48*, 466–475, doi:10.1080/00221686.2010.491649.

G. G. Katul, A. G. Konings, and S. E. Thompson, Nicholas School of the Environment, Duke University, Durham, NC 27708, USA. (konings@alum.mit.edu)